



Pharmacological characterization of the α_{2A} -adrenergic receptor inhibiting rat hippocampal CA3 epileptiform activity: comparison of ligand efficacy and potency

Joseph P. Biggane, Ke Xu, Brianna L. Goldenstein, Kylie L. Davis, Elizabeth J. Luger, Bethany A. Davis, Chris W.D. Jurgens, Dianne M. Perez, James E. Porter & Van A. Doze

To cite this article: Joseph P. Biggane, Ke Xu, Brianna L. Goldenstein, Kylie L. Davis, Elizabeth J. Luger, Bethany A. Davis, Chris W.D. Jurgens, Dianne M. Perez, James E. Porter & Van A. Doze (2022) Pharmacological characterization of the α_{2A} -adrenergic receptor inhibiting rat hippocampal CA3 epileptiform activity: comparison of ligand efficacy and potency, *Journal of Receptors and Signal Transduction*, 42:6, 580-587, DOI: [10.1080/10799893.2022.2110896](https://doi.org/10.1080/10799893.2022.2110896)

To link to this article: <https://doi.org/10.1080/10799893.2022.2110896>



© 2022 The Author(s). Published by Informa UK Limited, trading as Taylor & Francis Group.



[View supplementary material](#)



Published online: 19 Aug 2022.



[Submit your article to this journal](#)



Article views: 488



[View related articles](#)



[View Crossmark data](#)



Citing articles: 1 [View citing articles](#)

Pharmacological characterization of the α_{2A} -adrenergic receptor inhibiting rat hippocampal CA3 epileptiform activity: comparison of ligand efficacy and potency

Joseph P. Biggane^a, Ke Xu^a, Brianna L. Goldenstein^a, Kylie L. Davis^a, Elizabeth J. Luger^a, Bethany A. Davis^a, Chris W.D. Jurgens^a, Dianne M. Perez^b , James E. Porter^a and Van A. Doze^a 

^aDepartment of Biomedical Sciences, University of North Dakota School of Medicine and Health Sciences, Grand Forks, ND, USA;

^bDepartment of Cardiovascular & Metabolic Sciences, Lerner Research Institute, The Cleveland Clinic Foundation, Cleveland, OH, USA

ABSTRACT

The mechanism underlying the antiepileptic actions of norepinephrine (NE) is unclear with conflicting results. Our objectives are to conclusively delineate the specific adrenergic receptor (AR) involved in attenuating hippocampal CA3 epileptiform activity and assess compounds for lead drug development. We utilized the picrotoxin model of seizure generation in rat brain slices using electrophysiological recordings. Epinephrine (EPI) reduced epileptiform burst frequency in a concentration-dependent manner. To identify the specific receptor involved in this response, the equilibrium dissociation constants were determined for a panel of ligands and compared with established binding values for α_1 , α_2 , and other receptor subtypes. Correlation and slope of unity were found for the α_{2A} -AR, but not other receptors. Effects of different chemical classes of α -AR agonists at inhibiting epileptiform activity by potency (pEC₅₀) and relative efficacy (RE) were determined. Compared with NE (pEC₅₀, 6.20; RE, 100%), dexmedetomidine, an imidazoline (pEC₅₀, 8.59; RE, 67.1%), and guanabenz, a guanidine (pEC₅₀, 7.94; RE, 37.9%), exhibited the highest potency (pEC₅₀). In contrast, the catecholamines, EPI (pEC₅₀, 6.95; RE, 120%) and α -methyl-NE (pEC₅₀, 6.38; RE, 116%) were the most efficacious. These findings confirm that CA3 epileptiform activity is mediated solely by α_{2A} -ARs without activation of other receptor systems. These findings suggest a pharmacotherapeutic target for treating epilepsy and highlight the need for selective and efficacious α_{2A} -AR agonists that can cross the blood-brain barrier.

ARTICLE HISTORY

Received 3 June 2022

Revised 1 August 2022

Accepted 2 August 2022

KEYWORDS

α_{2A} -adrenergic receptor; antiepileptic; epilepsy; hippocampus; norepinephrine

Introduction

The noradrenergic system in the central nervous system (CNS) is characterized by a highly divergent projection of norepinephrine (NE)-containing fibers that originate from locus coeruleus neurons and radiate throughout the neuroaxis. Specificity in this system, where NE terminals are spread throughout the brain, is achieved through a diversity of adrenergic receptors (ARs) with distinct expression and functions. This diversity enables NE to regulate a number of critical neural functions including cognition and epileptogenesis [1].

The hippocampus, implicated in cognition, receives one of the highest densities of NE-containing terminals and is often involved in seizures, particularly with temporal lobe epilepsy, the most common form of epilepsy in adults. The high-seizure susceptibility of the hippocampus is believed due in part to the immense interconnectivity between hippocampal CA3 pyramidal neurons, known as recurrent circuitry. Due to the role of neuronal excitatory threshold in both seizure activity and activity-dependent synaptic plasticity, precise manipulation of the network activity in this region is essential to

effectively control seizures without interfering with cognition. Several studies suggest that the antiepileptic role of NE alters the epileptic circuit, rendering NE as a more-desirable drug target for disease modification in epilepsy, rather than current therapeutics that merely increase the threshold for seizures [1].

α -ARs are G protein-coupled receptors (GPCRs) that bind and transduce signals for NE and the hormone epinephrine (EPI). α_2 -AR (α_{2A} , α_{2B} , α_{2C}) and α_1 -AR subtypes (α_{1A} , α_{1B} , α_{1D}) are all expressed in the hippocampus [2–3]. The mechanism underlying the antiepileptic actions of NE is unclear with both agonists and antagonists of the same AR subtype reporting similar results and both α_1 - and α_2 -ARs contributing [4–9]. Although several centrally mediated actions are ascribed to α -ARs, the relative efficacy (RE) and potency of ligands at central α -ARs have not been extensively explored with respect to specific α -AR subtypes, contributing to difficulties in elucidating the CNS pharmacology of NE.

Previously, we presented evidence suggesting that α_{2A} -ARs mediate the antiepileptic effect of NE [10]. However, these findings were not definitive, as mRNA transcripts for

CONTACT Van A. Doze  van.doze@und.edu  Department of Biomedical Sciences, School of Medicine and Health Sciences, University of North Dakota, 1301 North Columbia Road Stop 9037, Grand Forks, ND 58202-9037, USA

 Supplemental data for this article can be accessed online at <https://doi.org/10.1080/10799893.2022.2110896>

© 2022 The Author(s). Published by Informa UK Limited, trading as Taylor & Francis Group.
This is an Open Access article distributed under the terms of the Creative Commons Attribution-NonCommercial-NoDerivatives License (<http://creativecommons.org/licenses/by-nc-nd/4.0/>), which permits non-commercial re-use, distribution, and reproduction in any medium, provided the original work is properly cited, and is not altered, transformed, or built upon in any way.

α_{2A} - and α_{2C} -ARs were also found in CA3 pyramidal cells [10] and several classes of GPCRs known to mediate CA3 epileptiform activity were not analyzed in that study [11–12]. Therefore, the involvement of other receptor systems remained a distinct possibility.

The first goal of this study was to conclusively delineate the specific receptor(s) involved in attenuating hippocampal epileptiform activity. The second objective of this investigation was to examine the RE and potency of various adrenergic agonists at inhibiting hippocampal CA3 epileptiform activity for future drug development. We also explore if age or gender influence this response as both are known factors in epileptic vulnerability [13–14].

Methods

Reagents

ARC-239, BRL-44408, clonidine hydrochloride, dexmedetomidine hydrochloride, efaroxan hydrochloride, guanabenz acetate, guanfacine hydrochloride, idazoxan hydrochloride, JP-1302, prazosin hydrochloride, rauwolscine hydrochloride, RS-79948, RX-821002, terazosin, UK-14304, WB-4101, and yohimbine hydrochloride were acquired from Tocris (Ellisville, MO). Atipamezole was from Orion Corporation (Espoo, Finland) and isoflurane was from Abbott Diagnostics (Chicago, IL). All other chemicals were obtained from Sigma-Aldrich (St. Louis, MO).

Animal use

Sprague-Dawley rats (31–200 d) weighing 90–300 g of both sexes were used and housed on a 12-h light/dark cycle in rooms maintained at a temperature of \sim 22 °C with a relative humidity of \sim 55%. Water and food were provided ad libitum. All protocols described have been approved by the Institutional Animal Care and Use Committee at the University of North Dakota in accordance with the *Guide for the Care and Use of Laboratory Animals* published by the National Institutes of Health.

Hippocampal slice preparation

Sprague-Dawley rats were anesthetized with isoflurane and sacrificed by decapitation. Brains were rapidly removed and the hippocampi quickly dissected from each hemisphere and placed into a 4 °C solution that contained 110 mM choline chloride, 2.5 mM KCl, 7 mM MgSO₄, 0.5 mM CaCl₂, 1.25 mM NaH₂PO₄, 25 mM NaHCO₃, 25 mM D-glucose, 11.6 mM sodium ascorbate, and 3.1 mM sodium pyruvate. Using a conventional tissue chopper, the hippocampi were sliced transversely into 500- μ m sections and transferred to artificial cerebral spinal fluid (ACSF) solution consisting of 119 mM NaCl, 5 mM KCl, 1.3 mM MgSO₄, 2.5 mM CaCl₂, 1 mM NaH₂PO₄, 26.2 mM NaHCO₃, and 11 mM D-glucose. The slices were incubated for 30 min at 34 °C, then transferred to room temperature (RT) and allowed to recover for at least 30 min. All solutions were continually aerated with 95% O₂, 5% CO₂.

Electrophysiological recordings

Microelectrodes were made from borosilicate glass using a PP-830 vertical two-stage puller (Narashige, Tokyo, Japan) and filled with 3 M NaCl. A slice was submerged in the recording chamber and perfused at a rate of \geq 4 ml/min with ACSF at RT. Using a SZ-61 stereo microscope (Olympus, Melville, NY) to visualize the CA3 region of the hippocampus, the microelectrode was placed in the center of *stratum pyramidale*. Extracellular field potentials were detected using either an Axoclamp 2B (Molecular Devices, Sunnyvale, CA) or BVC-700A (Dagan, Minneapolis, MN), amplified by a Brownlee 440 (Brownlee Precision, San Jose, CA), digitized with a Digidata 1322A (Molecular Devices), and recorded using Axoscope 9.0 software (Molecular Devices).

Generation of spontaneous epileptiform activity

Spontaneous epileptiform bursts were elicited by superfusing the slice with ACSF containing the GABA_A antagonist picrotoxin (100 μ M) to attenuate the synaptic inhibition (Figure 1(A)). If no burst discharges were seen after 30 min of perfusion, the slices were determined to be unresponsive and discarded. Once burst discharges were evident, 30 min of baseline data was recorded. The ACSF also contained desipramine (0.5 μ M) to block the potential reuptake of catecholamines and timolol (10 μ M) to block any β -AR-mediated effects. Some α_2 -AR ligands are known to possess potent 5-HT_{1A}-mediated agonist activity. For these AR ligands, pindolol (3 μ M) which blocks both β -AR and 5-HT_{1A} receptors was used in the place of timolol which only blocks β -ARs.

Epileptiform burst discharge frequencies were visualized in real time (Figure 1(B)) using Mini Analysis 6.0 software (Synaptosoft, Decatur, GA). Burst frequency was binned in the course of the experiment in 180-s intervals (Figure 1(C)). The last interval correlating to each agonist concentration was noted, baseline frequency was subtracted, and that value was used to plot a concentration–response curve expressed as percentage of maximal response (Figure 1(D)).

Experimental pK_b values for each α -AR ligand were determined using the method of Schild [15]. For each experiment, cumulative concentration–response curves were performed in hippocampal slices from the same rat (single concentration–response curve per slice). Dose-ratios of EC₅₀ values were calculated in the presence and absence of a α AR ligand and Schild regressions constructed. Linear regression analysis of these points was used to determine the slope and x-intercept of the Schild regressions.

Experimental pEC₅₀ values and RE were determined by measuring the change in response elicited by each α -AR ligand. The pEC₅₀ was calculated from the dose–response curve by non-linear regression analysis. The RE was calculated as the maximal response for each α -AR ligand normalized to the maximal response elicited by NE (i.e. 100), for comparisons of the maximal response between agonists and to allow comparisons to published data [16]. However, (–)EPI was used in experimental conditions to increase assay sensitivity due to its larger RE value (i.e. 120) compared with NE.

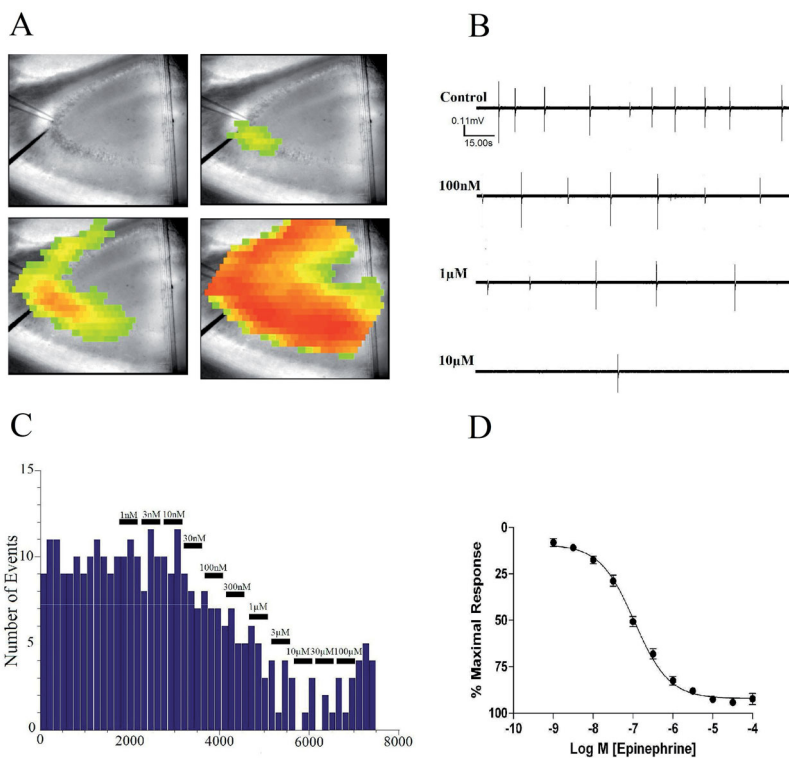


Figure 1. EPI reduces epileptiform burst discharge frequency. (A) Generation of hippocampal CA3 activity. Illustrated are pseudo-color images of a single epileptiform burst generated by voltage sensitive dye. (B) Continuous 150 s-long chart recordings of burst discharges are visualized on Axoscope 9.2. Increasing EPI produced a dose-dependent reduction of epileptiform burst activities. (C) Frequency histogram of burst discharges versus time of EPI administration. Each bin represents a 150-s time interval. (D) Concentration-response curve derived from 52 experiments.

Statistical methods

Concentration-response curves were constructed using a non-linear least squares curve fitting method in Prism (GraphPad, San Diego, CA). Each curve was fit with a standard (unity) or variable slope, and the best-fit determined using an *F*-test with a value of $p < 0.05$. Significance between groups was tested using an unpaired two-tailed Student's *t* test ($p < 0.05$).

Slopes are expressed as the mean \pm SE and the 95% confidence level used to conclude a significant difference between groups. Differences in pK_b values and Schild regression slopes were determined by analysis of covariance with a $p < 0.01$ level of probability as significant. Calculated pEC_{50} and pK_b values are expressed as the mean \pm SE for n experiments.

Results

Effects of EPI on hippocampal CA3 epileptiform activity

Under conditions of impaired synaptic inhibition by picrotoxin, CA3 pyramidal cells will spontaneously fire epileptiform burst discharges which will spread throughout the CA3 region. As illustrated in Figure 1(A), each burst discharge is characterized by a sharp biphasic spike that corresponds to the synchronous depolarization and hyperpolarization of a population of CA3 pyramidal cells. In the absence of α -AR blockade, application of EPI reduces the frequency of these events in a concentration-dependent manner without

affecting their amplitude (Figure 1(B)). Using a frequency histogram of the EPI-induced reduction in burst activity (Figure 1(C)), a concentration-response curve was constructed (Figure 1(D)). The mean EC_{50} for the EPI-induced decrease in burst frequency, derived from an aggregate of 52 experiments, was 108 ± 19 nM (Figure 1(D)).

Effects of selective α -AR ligands on EPI-mediated inhibition of epileptiform activity

To identify receptor involved in this response, the equilibrium dissociation constant (pK_b) of an α -AR ligand was functionally determined. Hippocampal slices that had been perfused with ACSF containing 3, 10, and 30 nM of RS-79948, a highly potent α_2 -AR antagonist [17], produced 4-, 13-, and 34-fold of parallel rightward shifts of the control EPI concentration-response curve (Figure 2(A)). The Schild regression slope included unity and the x-intercept of the regression line represent the RS-79948 pK_b of 9.00 ± 0.16 (Figure 2(B)). This pK_b corresponded closely to the affinity value of RS-79948 for α_2 -ARs (Table S1) and suggested that a α_2 -AR was mediating the effect of EPI on attenuating epileptiform burst discharge frequencies.

An assortment of α -AR ligands was then used to determine the specific subtype involved in this response and experimental pK_b values for these compounds were calculated. In all instances, ligands produced parallel rightward shifts of the fitted EPI concentration-response curve. Furthermore, the slope of the regression curve was unity for

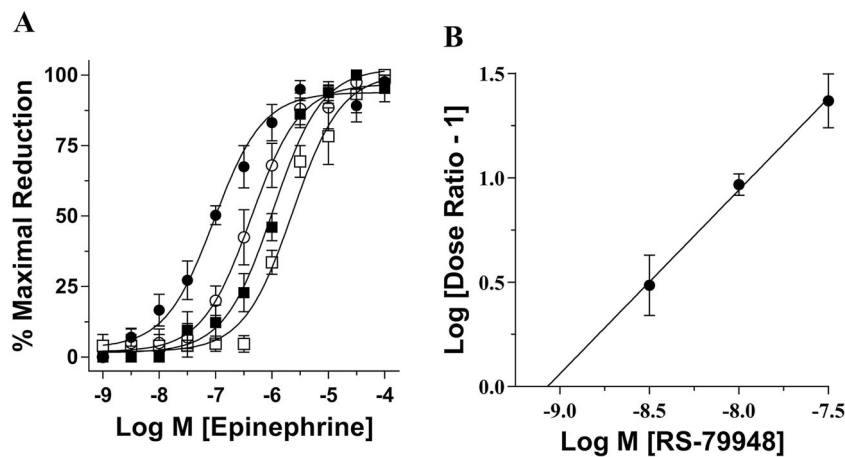


Figure 2. Schild regression analysis using a highly selective α_2 -AR antagonist. (A) Consecutive EPI concentration-response curves demonstrate a concentration-dependent effect of the selective α_2 -AR antagonist RS79948. Pretreatment with 3 nM (○), 10 nM (■), and 30 nM (□) of RS79948 produced consecutive parallel rightward shifts of the curve that were significantly different from control (●) ($EC_{50} = 423 \pm 148$ nM, 1211 ± 204 nM and 3221 ± 1954 nM, respectively, vs. 95 ± 16 nM for control). (B) Using dose ratios calculated from individual experiments illustrated in (A), a Schild plot was created generating a regression slope equaling 0.95 ± 0.11 and an x-intercept correlating to a pK_b value of 9.00 ± 0.16 ($n = 5$).

each of these compounds (Table S1). The calculated pK_b values of the α -AR ligands antagonizing EPI-induced reduction of epileptiform burst discharges were as follows: RS-79948 (9.00) > RX-821002 (8.87) > atipamezole (8.76) > efavoxan (8.43) > MK-912 (8.32) > phentolamine (8.16) > idazoxan (7.92) > BRL-44408 (7.81) > oxymetazoline (7.61) > rauwolscine (7.46) \geq naphazoline (7.42) = guanabenz (7.40) > WB-4101 (7.34) > xylometazoline (7.25) \geq yohimbine (7.20) > ARC-239 (6.14) > prazosin (5.31) = terazosin (5.30) \geq JP-1302 (5.23). We then correlated these experimental pK_b values with previously established pKi values for the rat and human α -AR subtypes (Table S1). There was a high correlation between our experimental pK_b values and the pKi values for both the rat α_{2A} -AR ($r = 0.99$, slope = 1.02, Figure 3(A)) and human α_{2A} -AR ($r = 0.93$, slope = 0.97, Figure 3(D)). In contrast, all other receptor subtypes showed either a lower correlation ($r \leq 0.90$) and/or a negative slope (Figure 3, Table S2).

Comparison of various classes of α -AR agonists normalized to percent maximal reduction of NE

To extend the relevance to possible human application, we then correlated our experimental pEC_{50} values with published pEC_{50} values of mouse and human α_2 -ARs, and human 5-HT_{1A} (Table S3). Although agonist responses such as potency and RE are system-dependent and may not reflect the same intracellular pathways and amplification effects, there was high correlation of the potency data to the human α_{2A} -AR subtype ($r = 0.92$) along with a slope of unity (Figure 3(E)). In contrast, for the human α_{2B} - or α_{2C} -AR, poor correlation coefficients were observed (Table S4). As imidazolines/guanidines can also cross-react with serotonergic receptors, we also compared published pEC_{50} with those of the 5-HT_{1A} subtype (Table S3). However, apart from oxymetazoline, imidazolines/guanidines displayed over 10–1000 fold lower potency for the 5-HT_{1A}, compared with the α_{2A} -AR, consistent with their low correlation (0.42) (Table S2).

Characterization of various AR agonists on attenuating epileptiform burst activities

We next examined the effects of various adrenergic agonists at inhibiting rat hippocampal CA3 epileptiform activity. AR agonists representing three chemical classes were tested and compared with the actions of NE. The rank order potency and RE values for the catecholamines were as follows: EPI ($EC_{50} = 72 \pm 18$ nM, RE = 1.20) > 6-FNE ($EC_{50} = 380 \pm 162$ nM, RE = 0.91) \geq α -methyl-NE ($EC_{50} = 417 \pm 199$ nM, RE = 1.16) > (–)-NE ($EC_{50} = 630 \pm 207$ nM, RE = 1.00) > deoxyNE ($EC_{50} = 3550 \pm 3400$ nM, RE = 1.00) > (+)-NE ($EC_{50} = 24000 \pm 7900$ nM, RE = 0.98) > phenylephrine ($EC_{50} = 107 \pm 148$ μ M, RE = 0.76) > isoproterenol ($EC_{50} = 182 \pm 51$ μ M, RE = 0.84). All catecholamines exhibited very high RE but relatively low potency when compared with other classes (Table S3, Figure 4(A)). In contrast, of the imidazolines and guanidines ligands, only UK-14304 was found to be a full agonist (≥ 0.75 RE) at a 79.2% relative efficacy to NE. All of the other imidazoline and guanidine ligands were partial agonists; however, most exhibited significantly higher potency than catecholamines (Figure 4(B)). The rank order potency and RE for the imidazolines and guanidines tested were as follows: dexmedetomidine ($EC_{50} = 2.57 \pm 1.56$ nM, RE = 0.67) > guanabenz ($EC_{50} = 11 \pm 10$ nM, RE = 0.40) \geq *p*-aminoclonidine ($EC_{50} = 13 \pm 13$ nM, RE = 0.32) > UK-14304 ($EC_{50} = 24 \pm 21$ nM, RE = 0.79) \geq oxymetazoline ($EC_{50} = 28 \pm 23$ nM, RE = 0.41) \geq xylometazoline ($EC_{50} = 33 \pm 36$ nM, RE = 0.20) > guanfacine ($EC_{50} = 49 \pm 46$ nM, RE = 0.45) > clonidine ($EC_{50} = 69 \pm 37$ nM, RE = 0.56) \gg xylazine ($EC_{50} = 6900 \pm 6200$ nM, RE = 0.27).

Effects of age and gender on the α_{2A} -AR properties of EPI

All data presented in this paper were collected in postnatal day (PND) from 12–30 rats, both male and female, with the exception of several from older age groups ranging from two to six month to determine the effects of age and gender on EPI's ability to reduce epileptiform burst activities in the hippocampus. The three age groups PND 12–30, PND

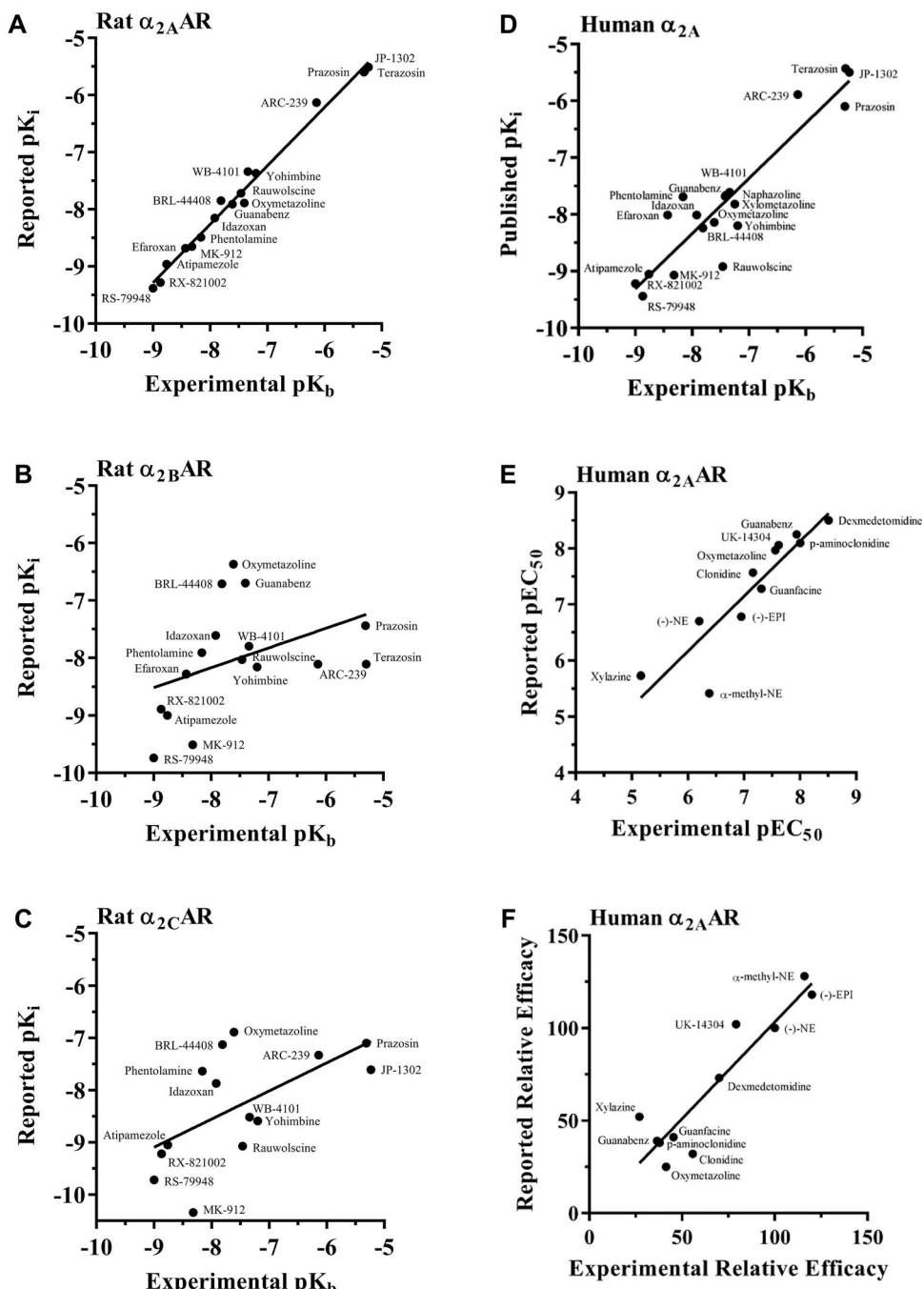


Figure 3. Correlation between experimental and reported pharmacological values for various α -AR ligands at rat or human α_2 A-ARs. Using the pK_i values in Table S1, correlation analyses were performed for the rat α_2 A- (A), α_2 B- (B), and α_2 C-AR (C), or using pK_b (D), pEC_{50} (E), or RE (F) at human α_2 A-ARs. The correlation coefficient and slope was 0.99 and 1.02, respectively, for the rat α_2 A-AR. A correlation coefficient and slope of 0.91 and 0.98, respectively, when correlating experimental pEC_{50} with the published human pEC_{50} for the α_2 A-AR. A correlation coefficient and slope of 0.92 and 1.05, respectively, when correlating experimental RE with the published human RE for the α_2 A-AR. Individual pK_b and pK_i values can be found in Table S1. Individual pEC_{50} and relative efficacy values are presented in Table S3. The slope and fit of each correlation are summarized in Tables S2 and S4.

60–120, and PND 121–200 all showed similar average pEC_{50} values and RE values with no statistically significant differences between any groups (Figure 5(A)). Similar comparisons were conducted with respect to gender (Figure 5(B)).

Discussion

In this study, we identified which AR mediates the inhibitory effect of NE on picrotoxin-induced rat hippocampal CA3 epileptiform activity and characterized various α -AR agonist

classes at this antiepileptic response. Although previous findings suggested that the α_2 A-AR was primarily mediating the antiepileptic action of NE, these results did not eliminate the possibility of effects due to α_2 C-AR, α_1 -AR, D₂, and 5-HT_{1A} [10]. This was mainly due to the low number of antagonists used in that study as well as the fact that α_2 A-AR mRNA expression level, used to identify the subtype, does not necessarily correlate to receptor protein function.

We addressed this problem by using a large number of α -AR ligands across receptor subtypes. In addition, we

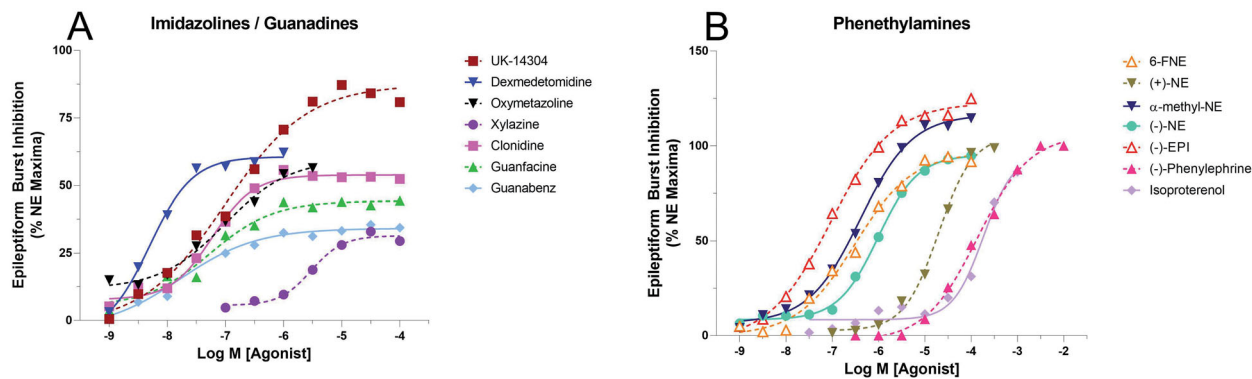


Figure 4. Comparison of various classes of α -AR agonists normalized to percent maximal reduction of NE on epileptiform burst inhibition. (A) The rank order potency for the imidazolines and guanadines is as follows: dexmedetomidine > guanabenz > UK-14304 > oxymetazoline > guanfacine > clonidine \gg xylazine. (B) The rank order potency for phenethylamines and their derivatives tested is as follows: EPI > 6-FNE \geq α -methyl-NE > $(-)$ - (R) -NE \gg $(+)$ - (S) -NE > $(-)$ -Phenylephrine > Isoproterenol.

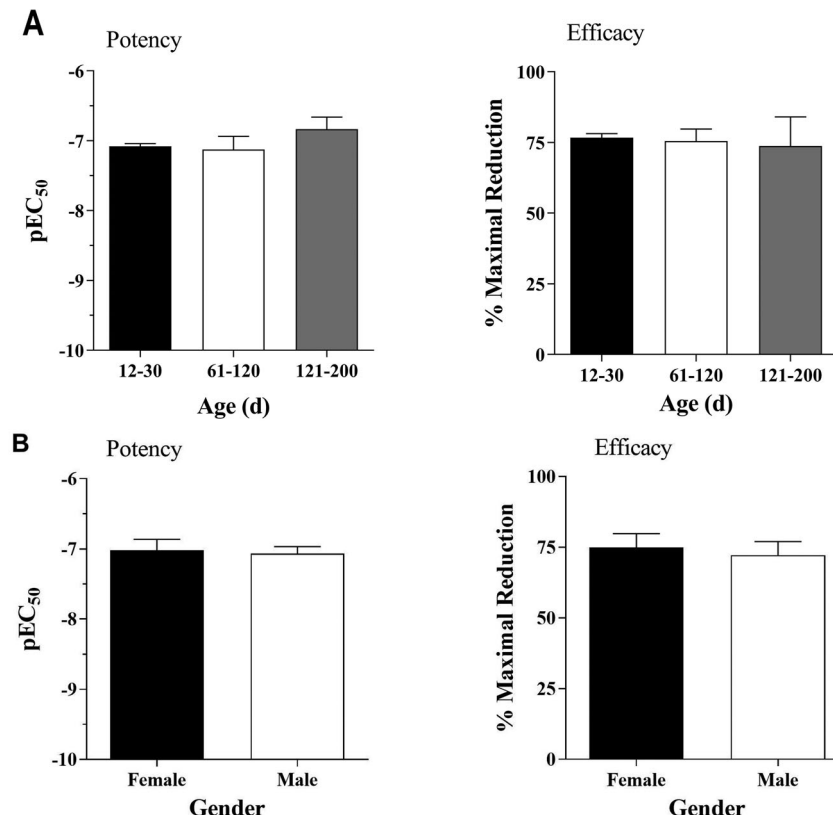


Figure 5. (A) Effects of age on the EPI-mediated inhibition of epileptiform activity. The average EC_{50} values for the PND12–30, 60–120, and 121–200 groups were 131 ± 10 nM ($n = 140$), 160 ± 70 nM ($n = 9$), and 204 ± 79 nM ($n = 8$), respectively. The average efficacy values for the three groups were $75 \pm 2\%$ ($n = 140$), $75 \pm 5\%$ ($n = 9$), and $73 \pm 9\%$ ($n = 7$), respectively. (B) Sex does not influence EPI-mediated inhibition of epileptiform activity. Age-matched average EC_{50} values are 93 ± 31 nM ($n = 13$) and 86 ± 19 nM ($n = 13$). Age-matched average efficacies are $75 \pm 4.9\%$ ($n = 13$), and $72 \pm 4.9\%$ ($n = 13$). Paired t -tests indicate no statistical significance in age or gender.

compiled a comprehensive list of binding (Table S1) and pEC_{50} (Table S3) profiles because many of the imidazolines/guanidines used in our study have affinities for other receptors, such as the 5-HT_{1A}. However, other than oxymetazoline which displays selectivity for human 5-HT_{1A}, all other imidazolines/guanidines displayed poor potency for 5-HT_{1A}. Activation of 5-HT_{1A} receptor has been shown to inhibit hippocampal network activity, although through an entirely different mechanism than that of α_{2A} -ARs, as 5-HT_{1A} activation leads to hyperpolarization of pyramidal cells, thereby inhibiting all neuronal activities [17]. This mechanism of inhibition

would not be an ideal therapeutic target for epilepsy since the absence of pyramidal cell activity would eliminate vital hippocampal functions such as cognition. In contrast, modulation of α_{2A} -AR by an agonist such as EPI does not hyperpolarize pyramidal cells (data not shown). Instead, we hypothesize that α_{2A} -AR activation reduces excess CA3 pyramidal cells recurrent network activity without interfering with normal transmission to and from the hippocampal CA3 region.

Using calculated pK_b for each ligand (Figure 2), a correlation study of all the receptor subtypes (Table S1) was

performed. As Table S2 indicates, the rat α_{2A} -AR exhibited near-perfect correlation with a slope and correlation coefficient of 1, whereas all other receptor subtypes showed very poor correlations. Our data indicate that the α_{2A} -AR is the sole mediator of the NE-mediated anti-epileptic action in the rat CA3 hippocampus. When the same correlation plot was also performed with respect to pK_i values from cloned human receptor subtypes (Table S2), the α_{2A} -AR exhibited a slope and r value of 0.97 and 0.93, respectively, which strengthens the applicability of our findings for therapeutic purposes in humans.

Upon resolving the identity of the receptor subtype, we next assess the most suitable agonist for lead drug development. We also tested different classes of AR agonists (catecholamine, imidazoline, guanidine) to evaluate their performance at inhibiting epileptiform burst activities with respect to NE (Figure 4). From a therapeutic standpoint, agonist(s) possessing the highest potency and efficacy would be the most promising candidate. Although most catecholamine compounds are expected to be full agonists, the imidazoline/guanidine agonists have little structural resemblance to catecholamines and therefore may interact with the α_2 -ARs through completely different mechanisms [18–19]. However, unlike catecholamines, most imidazolines/guanidines can cross the blood–brain barrier, which is critical when considering their potential role in drug therapies. Rank order potency revealed that the imidazolines/guanidines possessed the highest pEC_{50} values (Figure 4(B)), as the most potent imidazoline, dexmedetomidine, is over 30-fold more potent than EPI, the most potent catecholamine. However, all catecholamines were full agonists while only one non-catecholamine, UK-14304 (RE = 79.2), was a full agonist in this system (Figure 4(A)).

To better address the relevance of our findings with clinical applications, we compared our experimental EC_{50} values with published EC_{50} for cloned human α_2 -ARs (Table S3). The most efficacious, potent, and subtype selective agonist with the ability to cross the blood–brain barrier would be the ideal candidate for clinical application. Catecholamines had excellent efficacy (Figure 4(A), Table S3), but none can cross the blood–brain barrier because of a highly charged protonated amine. The most potent agonists either had no subtype selectivity (dexmedetomidine), or had very poor efficacy (guanabenz, oxymetazoline) (Figure 4(B), Table S3). UK-14304 is the only agonist which exhibited moderate efficacy and potency, some subtype selectivity (10-fold greater potency at α_{2A} -ARs than α_{2B} - or α_{2C} -ARs), and a 1,000-fold lower potency toward 5-HT_{1A}. Even so, the clinical applicability of UK-14304 is not ideal because, as with all non-catecholamines, the consistency of this agonist was not as high as catecholamines. EPI produced consistent effects that gave sigmoidal curves with little variance. In contrast, UK-14304 curves were often not sigmoidal and its potency and efficacy had large standard deviations (Table S3). It has been hypothesized and now shown in crystal structures that imidazolines activate ARs differently than catecholamines [18,20–23], which would account for the irregularities we have observed. In particular, F427^{7,39}, a key residue in α_{2A} -AR activation and identified as

a ‘switching lid’ of an aromatic cage [22], makes stronger contacts to the imidazoline ring than the amino-ethyl of NE [23], which contributes to imidazoline efficacy and subtype selectivity. Distinguishing UK-14304 from dexmedetomidine, the bicyclic aromatic moiety of UK-14304 interacts stronger than dexmedetomidine with Y409^{6,55}, another key residue involved in α_{2A} -AR activation, and suggested to play a role in pathway-specific signaling similar to NE [23]. In conjunction with UK-14304 being α_{2A} -AR subtype selective while dexmedetomidine is not, chemical derivation of UK-14304 may produce a more ideal clinical candidate that preserves NE-specific antiepileptic function. Although imidazolines in general impart better potency than catecholamines because of higher binding affinities to α_2 -ARs (i.e. affinity-driven agonists), incorporating efficacy in the assessment [24] provides the best guide to derivation of UK-14304, as both subtype-selectivity as well as full agonism would be the ideal antiepileptic therapeutic.

Finally, we explored age and gender as both parameters are associated with higher incidence of epilepsy [13–14]. However, our data suggest that age and gender do not significantly influence the potency or efficacy of EPI (Figure 5). As low efficacy, signaling-bias, and pregnancy/menopause may induce changes in pharmacokinetics [25] that influence age and gender responses to therapeutics, our conclusions are limited and cannot be translated to other drugs such as the imidazolines/guanidines.

The functional CNS model of analysis performed here is seldom used, which is one of the factors that led to a disproportional understanding of AR in the periphery than in the CNS. Our *in situ* functional model offers an unique outlook on AR agonist functions rarely explored by *in vitro* models such as [³⁵S]GTP γ S binding by Jasper *et al.* [19]. Although this study reported a comprehensive list of pEC_{50} values for a large number of compounds, the absence of a relatable physiological function remains a major drawback. Because of the nature of the methods, system specificity cannot be easily achieved by conventional *in vivo* and *in vitro* models. Therefore, separation and retention of the complete hippocampal CA3 circuitry *in situ* are one of our primary strengths, which allowed us to study the pharmacology of the α -AR system as a whole.

In summary, the α_{2A} -AR was determined to be the sole AR subtype mediating EPI-inhibition of rat hippocampal CA3 epileptiform activity and activity was neither gender nor age-dependent. Compared with established binding (pK_i) values for the rat and human receptors, our data also suggest that the α_{2A} -AR is a promising target for attenuating human hippocampal CA3 epileptiform activity. Generation of highly selective, efficacious, and brain-penetrant agonists for the α_{2A} -AR based upon the UK-14304 pharmacophore could provide novel therapeutic strategies for treating temporal lobe epilepsy.

Acknowledgements

The authors thank Sarah J. Boese, Jasmine J. O’Brien, Jackie L. Pribula, and Christina L. Schulte for assistance with experiments during their

summer research experiences, and Dr. Rory McQuiston for assistance with the voltage sensitive dye images.

Disclosure statement

No potential conflict of interest was reported by the authors.

Funding

This research was supported by a University of North Dakota School of Medicine and Health Sciences Undergraduate Research Fellowship (J.A.P.), a National Science Foundation (NSF) Graduate Research Fellowship DGE-0950693 (B.L.G.), NSF Research Experiences for Undergraduates Site grants 0851869 (K.L.D., E.J.L., V.A.D.) and 1359243 (V.A.D.), an Institutional Development Award from the National Institute of General Medical Sciences P20-GM103442 (V.A.D.), a National Institute of Aging R01-AG066627 (D.M.P.) and The Edward N. & Della L. Thome Memorial Foundation Awards Program in Alzheimer's Disease Drug Discovery Research (D.M.P.).

ORCID

Dianne M. Perez  <http://orcid.org/0000-0002-1790-5776>
Van A. Doze  <http://orcid.org/0000-0002-5288-9564>

Data availability statement

Supplemental data sets are directly available in this manuscript or by contacting the corresponding author, Dr. Van Doze.

References

- [1] Giorgi FS, Pizzanelli C, Biagioli F, et al. The role of norepinephrine in epilepsy: from the bench to the bedside. *Neurosci Biobehav Rev*. **2004**;28(5):507–524.
- [2] Hapke HK, Coulter CL, Gerety ME, et al. α_2 -adrenergic receptor development in rat CNS: an autoradiographic study. *Neuroscience*. **2004**;123(1):167–178.
- [3] Zilles K, Gross G, Schleicher A, et al. Regional and laminar distributions of alpha1-adrenoceptors and their subtypes in human and rat hippocampus. *Neuroscience*. **1991**;40(2):307–320.
- [4] Weinshenker D, Szot P. The role of catecholamines in seizure susceptibility: new results using genetically engineered mice. *Pharmacol Ther*. **2002**;94(3):213–233.
- [5] Clinckers R, Zgavc T, Vermoesen K, et al. Pharmacological and neurochemical characterization of the involvement of hippocampal adrenoreceptor subtypes in the modulation of acute limbic seizures. *J Neurochem*. **2010**;115(6):1595–1607.
- [6] Ghasemi M, Mehranfar N. Mechanisms underlying anticonvulsant and proconvulsant actions of norepinephrine. *Neuropharmacology*. **2018**;137:297–308.
- [7] Iváñez V, Ojeda J. Exacerbation of seizures in medial temporal lobe epilepsy due to an alpha1-adrenergic antagonist. *Epilepsia*. **2006**;47(10):1741–1742.
- [8] Löscher W, Czuczwar SJ. Comparison of drugs with different selectivity for Central alpha1- and alpha2-adrenoceptors in animal models of epilepsy. *Epilepsy Res*. **1987**;1(3):165–172.
- [9] Weinshenker D, Szot P, Miller NS, et al. Alpha(1) and beta(2)-adrenoceptor agonists inhibit pentylenetetrazole-induced seizures in mice lacking norepinephrine. *J Pharmacol Exp Ther*. **2001**;298(3):1042–1048.
- [10] Jurgens CWD, Hammad HM, Lichter JA, et al. α_{2A} adrenergic receptor activation inhibits epileptiform activity in the rat hippocampal CA3 region. *Mol Pharmacol*. **2007**;71(6):1572–1581.
- [11] Gill CH, Soffin EM, Hagan JJ, et al. 5-HT₇ receptors modulate synchronized network activity in rat hippocampus. *Neuropharmacology*. **2002**;42(1):82–92.
- [12] Tesson F, Limon-Boulez I, Urban P, et al. Localization of I2-imidazoline binding sites on monoamine oxidases. *J Biol Chem*. **1995**;270(17):9856–9861.
- [13] Hauser WA. Seizure disorders: the changes with age. *Epilepsia*. **1992**;33 Suppl 4(Suppl 4):S6–S14.
- [14] Savic I. Sex differences in human epilepsy. *Exp Neurol*. **2014**;259:38–43.
- [15] Arunlakshana O, Schild HO. Some quantitative uses of drug antagonists. *Br J Pharmacol Chemother*. **1959**;14(1):48–58.
- [16] Uhlén S, Dambrova M, Näsman J, et al. 3H]RS79948-197 binding to human, rat, guinea pig and pig α_{2A} -, α_{2B} - and α_{2C} -adrenoceptor. Comparison with MK912, RX821002, rauwolscine and yohimbine. *Eur J Pharmacol*. **1998**;343(1):93–101.
- [17] Beck SG, Choi KC, List TJ. Comparison of 5-hydroxytryptamine_{1A}-mediated hyperpolarization in CA1 and CA3 hippocampal pyramidal cells. *J Pharmacol Exp Ther*. **1992**;263(1):350–359.
- [18] Ruffolo RR, Jr, Rice PJ, Patil PN, et al. Differences in the applicability of the easson-stedman hypothesis to the alpha1- and alpha2-adrenergic effects of phenethylamines and imidazolines. *Eur J Pharmacol*. **1983**;86(3-4):471–475.
- [19] Jasper JR, Lesnick JD, Chang LK, et al. Ligand efficacy and potency at recombinant α_2 -adrenergic receptors: agonist-mediated [35S]GTP γ S binding. *Biochem Pharmacol*. **1998**;55(7):1035–1043.
- [20] Chen X, Xu Y, Qu L, et al. Molecular mechanism for ligand recognition and subtype selectivity of α_{2C} -Adrenergic receptor. *Cell Rep*. **2019**;29(10):2936–2943.e4.
- [21] Yuan D, Liu Z, Kaindl J, et al. Activation of the α_{2B} -adrenoceptor by the sedative sympatholytic dexamethadomidine. *Nat Chem Biol*. **2020**;16(5):507–512.
- [22] Qu L, Zhou Q, Xu Y, et al. Structural basis of the diversity of adrenergic receptors. *Cell Rep*. **2019**;29(10):2929–2935.e4.
- [23] Xu J, Cao S, Hübner H, et al. Structural insights into ligand recognition, activation, and signaling of the α_{2A} adrenergic receptor. *Sci Adv*. **2022**;8(9)eabj:5347.
- [24] Strange PG. Agonist binding, agonist affinity and agonist efficacy at G protein-coupled receptors. *Br J Pharmacol*. **2008**;153(7):1353–1363.
- [25] Soldin OP, Mattison DR. Sex differences in pharmacokinetics and pharmacodynamics. *Clin Pharmacokinet*. **2009**;48(3):143–157.